T★AFSM

Space–Time Computational FSI Techniques

Kenji Takizawa
Waseda University

Tayfun E. Tezduyar
Rice University

Happy 60th Birthday, Tony!

FSI Modeling of Spacecraft Parachutes

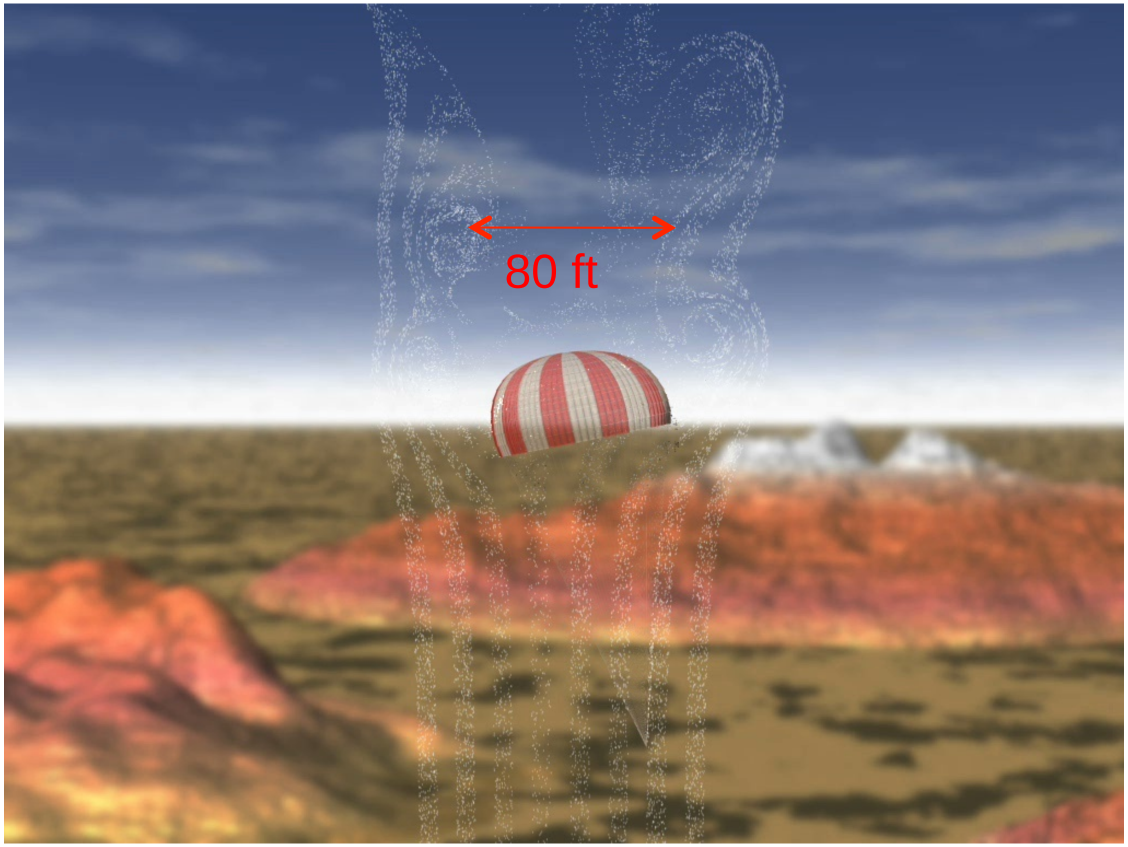

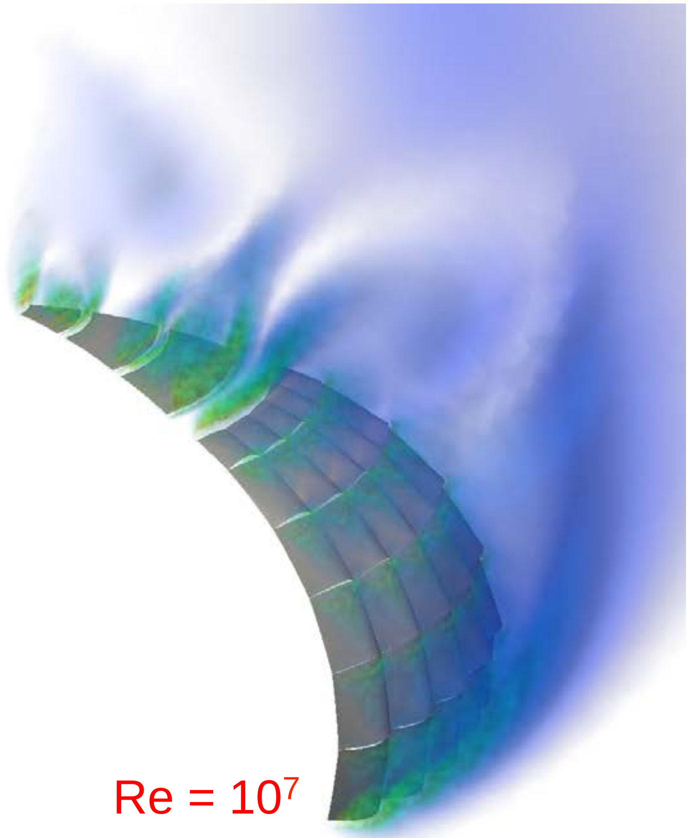

- Parachute structure is light and sensitive to changes in fluid forces.
- Ringsail parachutes have hundreds of gaps and slits.
- Parachutes are used in clusters, with contact between them.
- Parachute operation involves disreefing from one stage to next.

Flapping-Wing Aerodynamics of an Actual Locust

Video-Captured Data

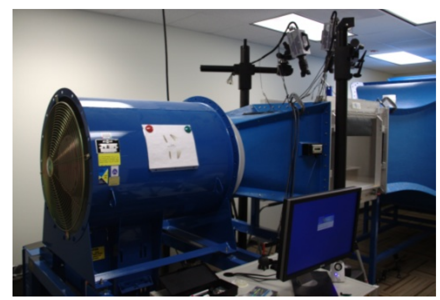

Dr. Fabrizio Gabbiani and Dr. Raymond Chan (BCM, Houston)

Flapping-Wing Aerodynamics of an Actual Locust

Computational Results

45 mm

Flapping: 20 Hz

- Correct lift force calculation requires correct flapping motion.
- The computational domain has near topology changes in a flapping cycle.

WIAS RICE

Deforming-Spatial-Domain/Stabilized Space–Time Formulation (DSD/SST) (ST-SUPS)

$$\int_{Q_n} \mathbf{w}^h \cdot \rho \left(\frac{\partial \mathbf{u}^h}{\partial t} + \mathbf{u}^h \cdot \boldsymbol{\nabla} \mathbf{u}^h - \mathbf{f}^h \right) dQ + \int_{Q_n} \boldsymbol{\varepsilon}(\mathbf{w}^h) : \boldsymbol{\sigma}(p^h, \mathbf{u}^h)\, dQ - \int_{(P_n)_\mathrm{h}} \mathbf{w}^h \cdot \mathbf{h}^h\, dP$$

$$+ \int_{Q_n} q^h \boldsymbol{\nabla} \cdot \mathbf{u}^h\, dQ + \int_{\Omega_n} (\mathbf{w}^h)_n^+ \cdot \rho \left((\mathbf{u}^h)_n^+ - (\mathbf{u}^h)_n^- \right) d\Omega$$

$$+ \sum_{e=1}^{(n_{el})_n} \int_{Q_n^e} \frac{1}{\rho} \left[\tau_{\mathrm{SUPG}} \rho \left(\frac{\partial \mathbf{w}^h}{\partial t} + \mathbf{u}^h \cdot \boldsymbol{\nabla} \mathbf{w}^h \right) + \tau_{\mathrm{PSPG}} \boldsymbol{\nabla} q^h \right] \cdot \left[\mathrm{L}(p^h, \mathbf{u}^h) - \rho \mathbf{f}^h \right] dQ$$

$$+ \sum_{e=1}^{(n_{el})_n} \int_{Q_n^e} \nu_{\mathrm{LSIC}} \boldsymbol{\nabla} \cdot \mathbf{w}^h \rho \boldsymbol{\nabla} \cdot \mathbf{u}^h\, dQ = 0$$

$$\mathrm{L}(q^h, \mathbf{w}^h) = \rho \left(\frac{\partial \mathbf{w}^h}{\partial t} + \mathbf{u}^h \cdot \boldsymbol{\nabla} \mathbf{w}^h \right) - \boldsymbol{\nabla} \cdot \boldsymbol{\sigma}(q^h, \mathbf{w}^h)$$

DSD/SST

ST Slab

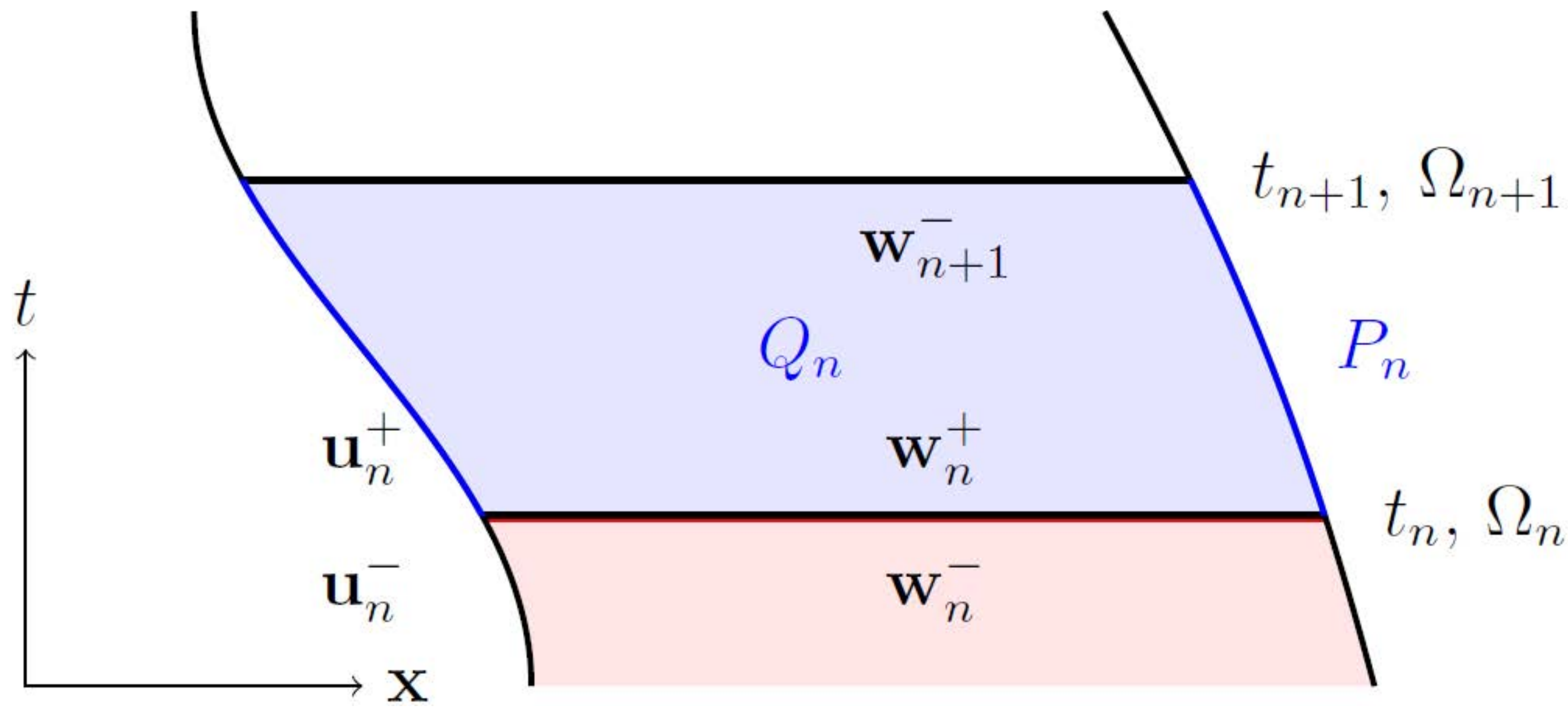

ST Finite Element

$$N_a^\alpha = T^\alpha(\theta)\, N_a(\boldsymbol{\xi}), \quad a = 1, 2, \ldots, n_{en}, \\ \alpha = 1, 2, \ldots, n_{ent},$$

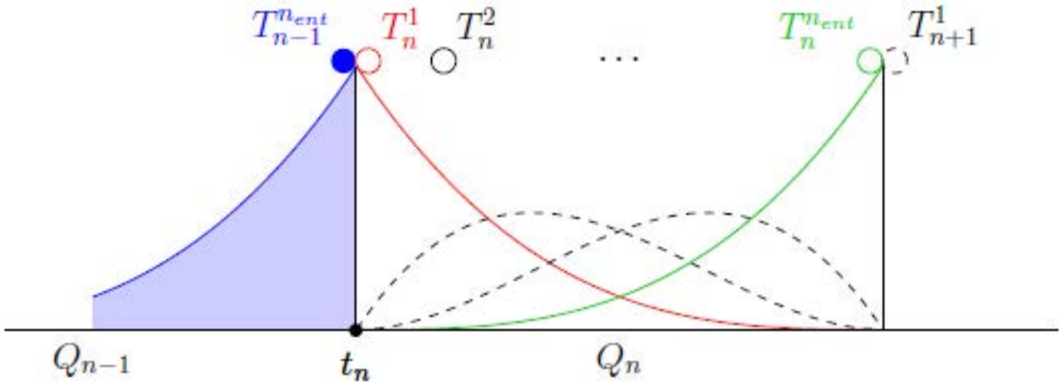

- High spatial and temporal accuracy
- Advantages in space–time framework

ST-VMS (DSD/SST-VMST) Method

Advective Form

$$
\begin{aligned}
&\int_{Q_n} \mathbf{w}^h \cdot \rho \left(\frac{\partial \mathbf{u}^h}{\partial t} + \mathbf{u}^h \cdot \boldsymbol{\nabla} \mathbf{u}^h - \mathbf{f}^h \right) dQ + \int_{Q_n} \boldsymbol{\varepsilon}(\mathbf{w}^h) : \boldsymbol{\sigma}(p^h, \mathbf{u}^h) dQ \\
&- \int_{(P_n)_\mathrm{h}} \mathbf{w}^h \cdot \mathbf{h}^h dP + \int_{Q_n} q^h \boldsymbol{\nabla} \cdot \mathbf{u}^h dQ + \int_{\Omega_n} (\mathbf{w}^h)_n^+ \cdot \rho \left((\mathbf{u}^h)_n^+ - (\mathbf{u}^h)_n^- \right) d\Omega \\
&- \sum_{e=1}^{(n_{el})_n} \int_{Q_n^e} \left[\rho \left(\frac{\partial \mathbf{w}^h}{\partial t} + \mathbf{u}^h \cdot \boldsymbol{\nabla} \mathbf{w}^h \right) + \boldsymbol{\nabla} q^h \right] \cdot \mathbf{u}' dQ - \sum_{e=1}^{(n_{el})_n} \int_{Q_n^e} \boldsymbol{\nabla} \cdot \mathbf{w}^h p' dQ \\
&+ \sum_{e=1}^{(n_{el})_n} \int_{Q_n^e} \mathbf{w}^h \cdot \rho (\mathbf{u}' \cdot \boldsymbol{\nabla} \mathbf{u}^h) dQ - \sum_{e=1}^{(n_{el})_n} \int_{Q_n^e} \rho \mathbf{u}' \cdot (\boldsymbol{\nabla} \mathbf{w}^h) \cdot \mathbf{u}' dQ = 0
\end{aligned}
$$

Terms existed in ST-SUPS

Terms added in ST-VMS

FSI Modeling of Spacecraft Parachutes

ST-SUPS

- Large displacements
- Near contact
- Near topology changes
- “Nearness” is sufficiently “near” for the purpose of solving this problem

Flapping-Wing Aerodynamics of an Actual Locust

ST-VMS

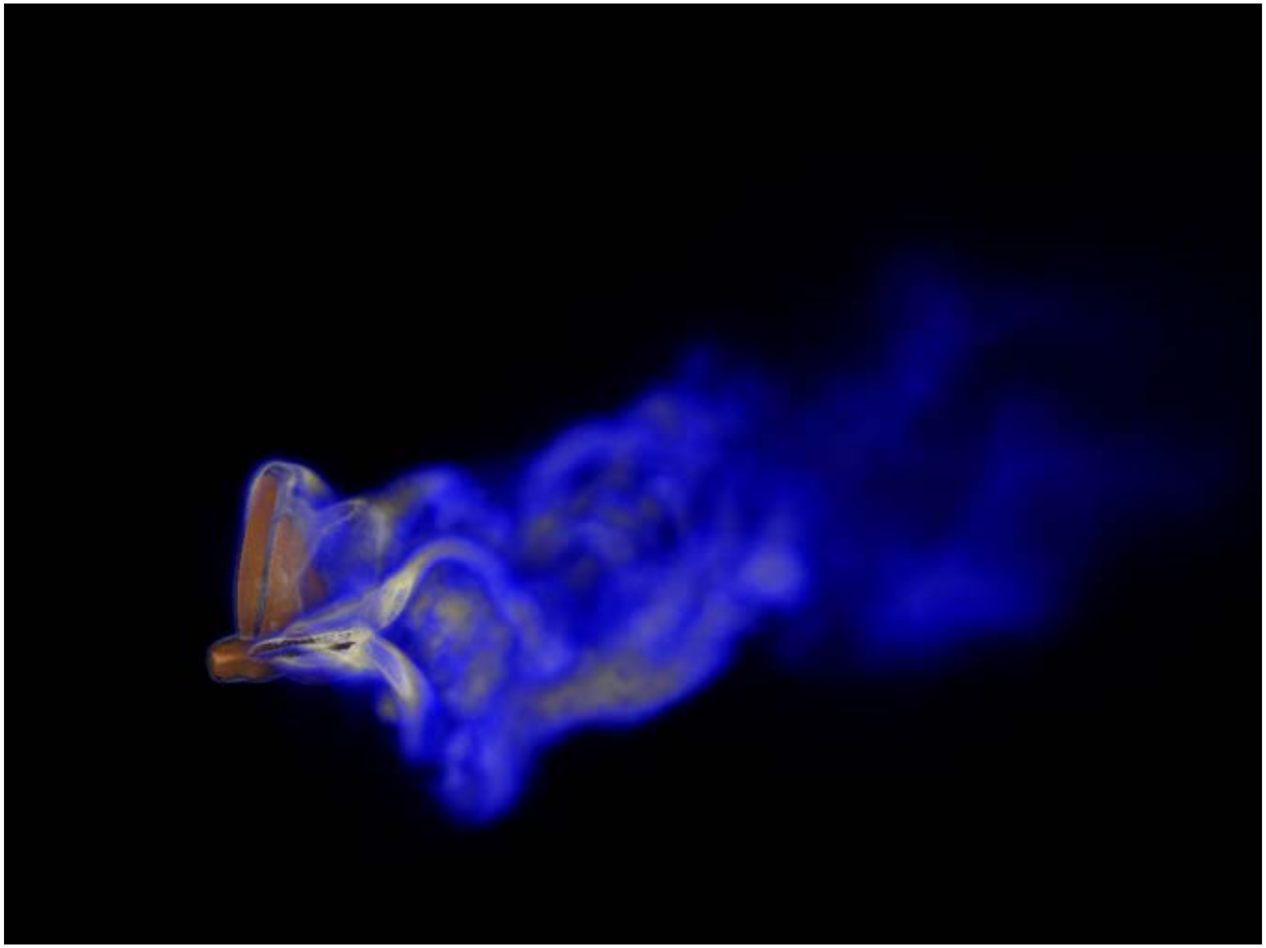

- Large displacements
- Near topology changes

Mixed Interface-Tracking/Interface-Capturing Technique (MITICT)

T. Tezduyar, "Finite element methods for flow problems with moving boundaries and interfaces", *Archives of Computational Methods in Engineering*, **8** (2001) 83–130.

- Track the fluid–solid interfaces with a moving mesh.
- Capture over that moving mesh the fluid–fluid interfaces you cannot track.

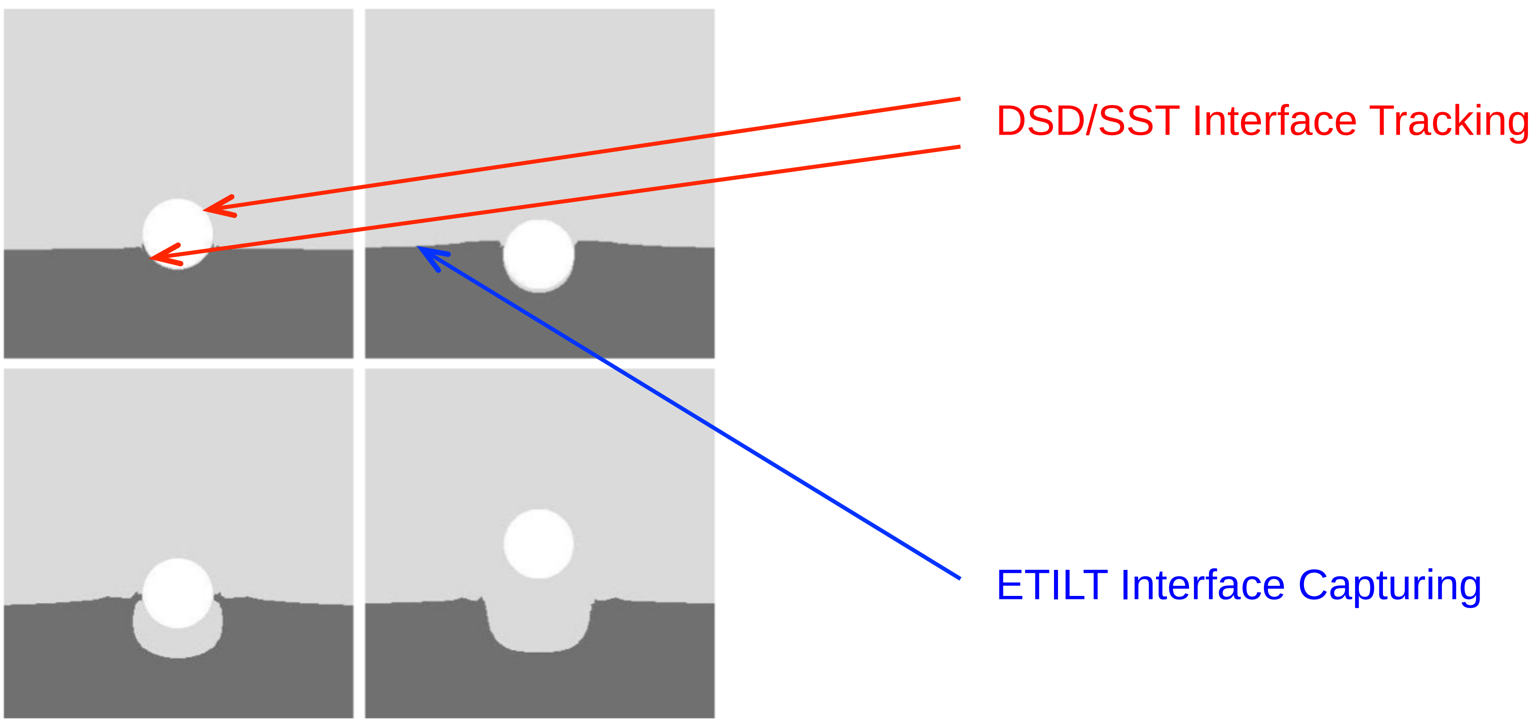

J.E. Akin, T. Tezduyar and M. Ungor, "Computation of flow problems with the Mixed Interface-Tracking/Interface-Capturing Technique (MITICT)", *Computers & Fluids*, **36** (2007) 2–11.

Fluid–Solid Interface-Tracking/Interface-Capturing Technique (FSITICT)

T. Tezduyar, K. Takizawa, C. Moorman, S. Wright, and J. Christopher, "Space–time finite element computation of complex fluid–structure interactions", *International Journal for Numerical Methods in Fluids*, **64** (2010) 1021–1218.

- Track the interfaces you can with a moving mesh.
- Capture over that moving mesh the interfaces you cannot track.

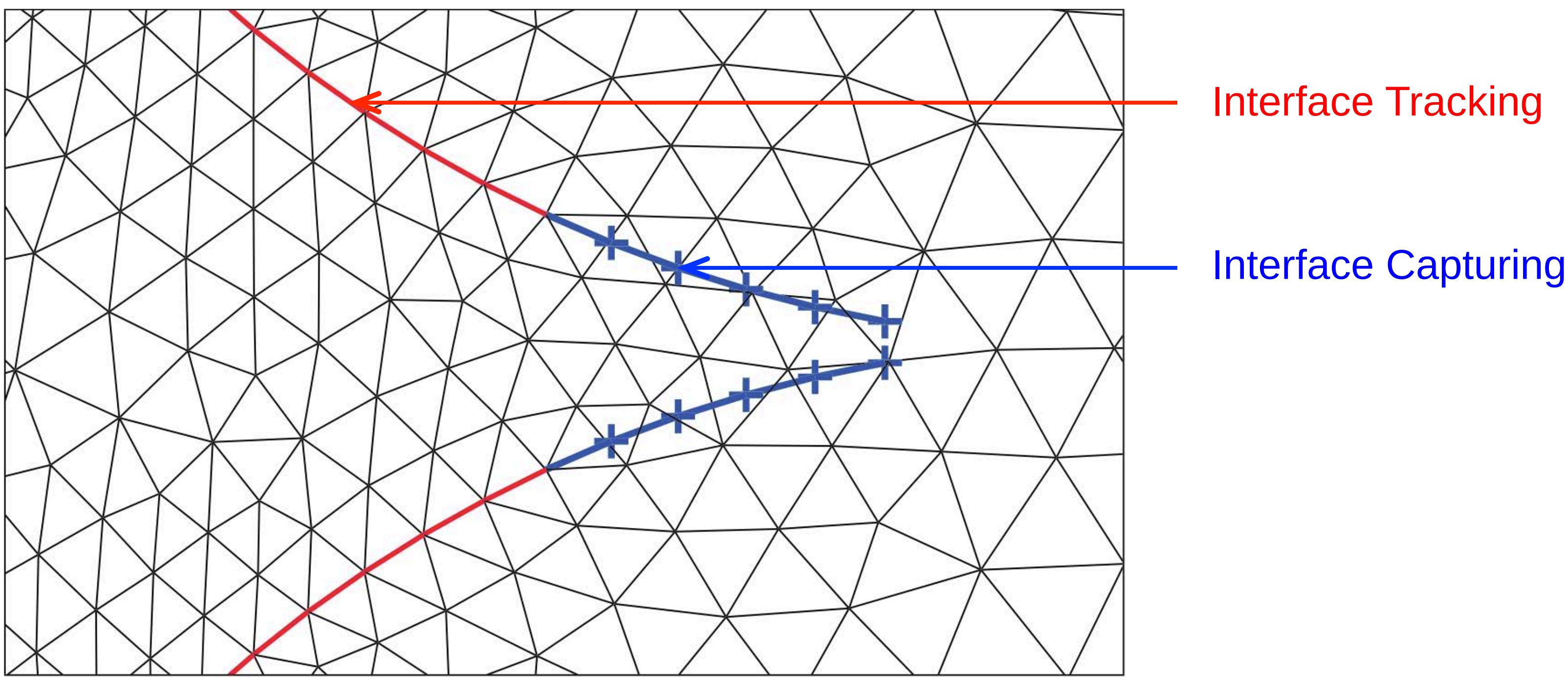

Method Supreme

Has the…

- Accuracy of interface-tracking (moving-mesh) methods
  Better resolution of boundary layers

- Flexibility of being able to deal with TC in the fluid mechanics mesh
  Allow actual contact between moving solid surfaces

- Computational practicality of accomplishing these in 3D analysis
  Realistic meshes and computing times

ST Interface-Tracking with Topology Change (ST-TC)

Method Supreme

Next Presentation: Kenji Takizawa

Solution of Fully-Discretized Equations

$$
\begin{aligned}
\text{Fluid} &\longrightarrow \mathbf{N}_1\left(\mathbf{d}_1, \mathbf{d}_2, \mathbf{d}_3\right) = \mathbf{F}_1 \\
\text{Structure} &\longrightarrow \mathbf{N}_2\left(\mathbf{d}_1, \mathbf{d}_2, \mathbf{d}_3\right) = \mathbf{F}_2 \\
\text{Mesh} &\longrightarrow \mathbf{N}_3\left(\mathbf{d}_1, \mathbf{d}_2, \mathbf{d}_3\right) = \mathbf{F}_3
\end{aligned}
$$

Mesh

Fluid Structure

Solution of Fully-Discretized Equations

Block-Iterative Coupling

$$\left.\frac{\partial \mathbf{N}_1}{\partial \mathbf{d}_1}\right|_{\left(\mathbf{d}_1^i,\ \mathbf{d}_2^i,\ \mathbf{d}_3^i\right)} \left(\Delta \mathbf{d}_1^i\right) \ = \ \mathbf{F}_1 - \mathbf{N}_1\left(\mathbf{d}_1^i,\ \mathbf{d}_2^i,\ \mathbf{d}_3^i\right)$$

$$\boxed{\left.\frac{\partial \mathbf{N}_2}{\partial \mathbf{d}_2}\right|_{\left(\mathbf{d}_1^{i+1},\ \mathbf{d}_2^i,\ \mathbf{d}_3^i\right)}} \left(\Delta \mathbf{d}_2^i\right) \ = \ \mathbf{F}_2 - \mathbf{N}_2\left(\mathbf{d}_1^{i+1},\ \mathbf{d}_2^i,\ \mathbf{d}_3^i\right))$$

$$\left.\frac{\partial \mathbf{N}_3}{\partial \mathbf{d}_3}\right|_{\left(\mathbf{d}_1^{i+1},\ \mathbf{d}_2^{i+1},\ \mathbf{d}_3^i\right)} \left(\Delta \mathbf{d}_3^i\right) \ = \ \mathbf{F}_3 - \mathbf{N}_3\left(\mathbf{d}_1^{i+1},\ \mathbf{d}_2^{i+1},\ \mathbf{d}_3^i\right)$$

Flow-Induced Vibrations of a Cantilevered Pipe

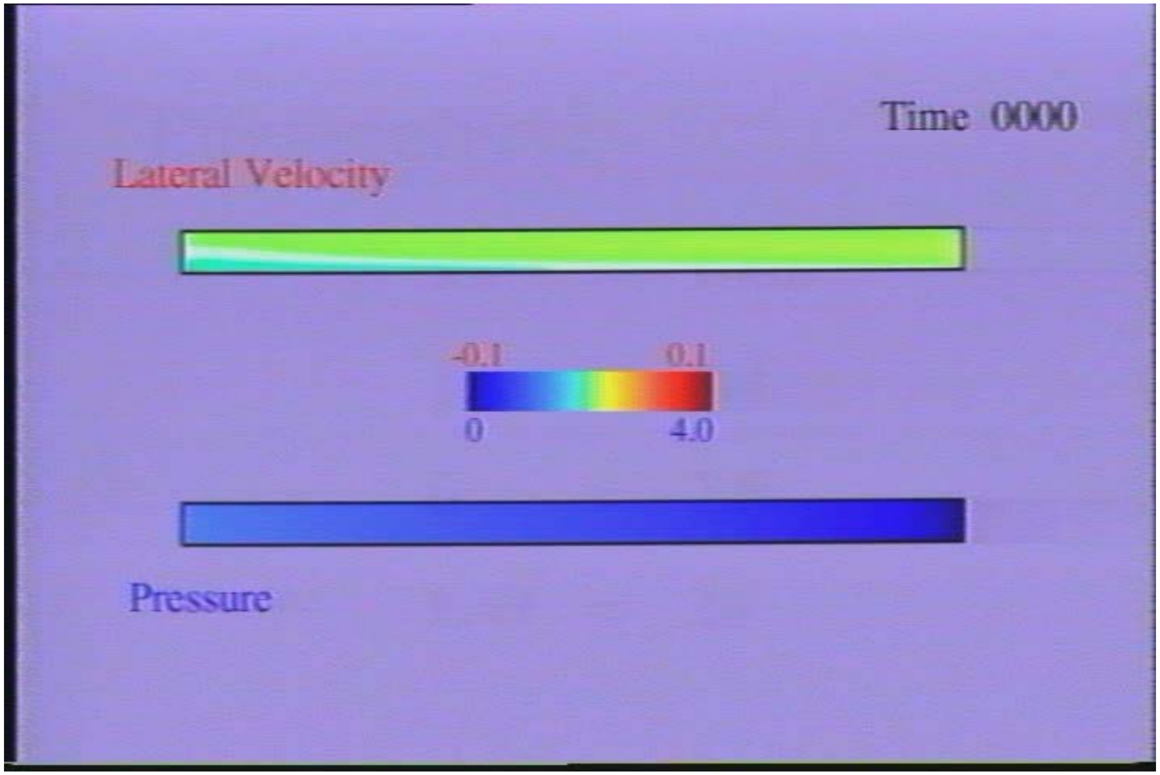

S. Mittal and T.E. Tezduyar, "Parallel finite element simulation of 3D incompressible flows – fluid-structure interactions", *International Journal for Numerical Methods in Fluids*, 21 (1995) 933-953.

FSI Modeling of a Parachute PMA Retraction

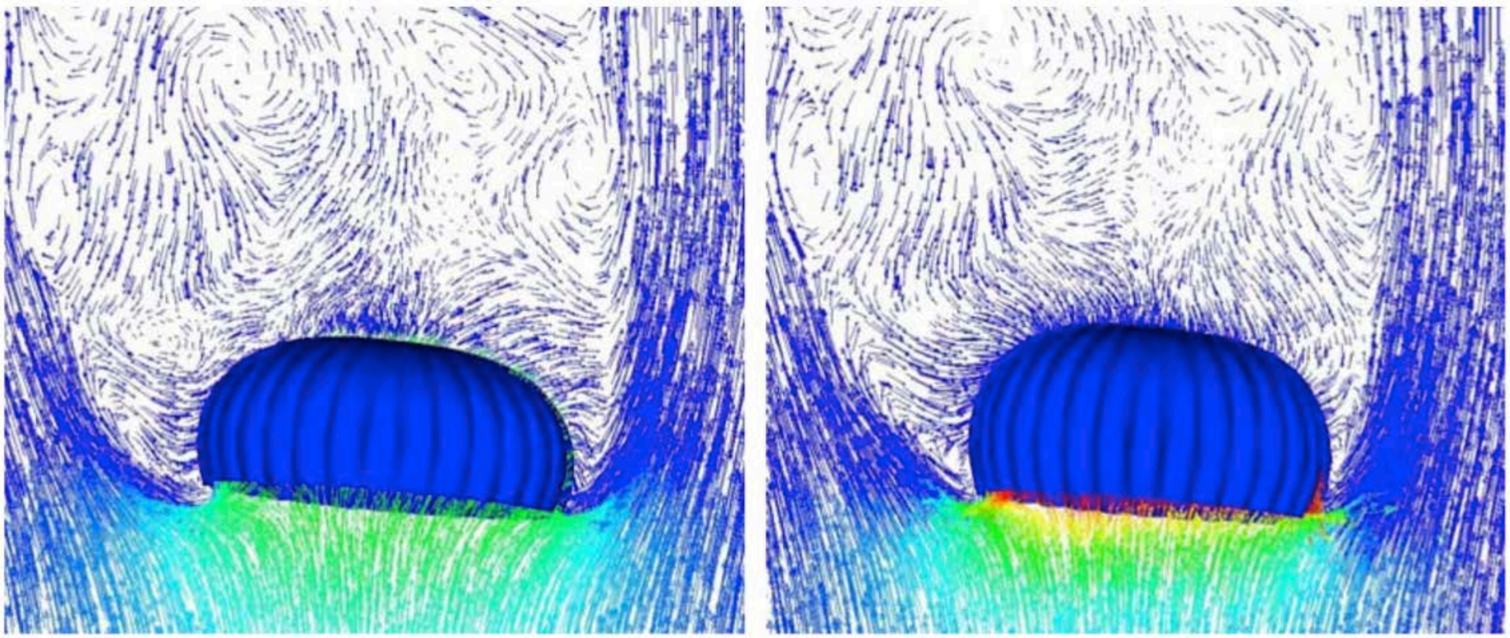

Before Retraction After Retraction

T.E. Tezduyar, S. Sathe, R. Keedy and K. Stein, "Space–time finite element techniques for computation of fluid–structure Interactions", *Computer Methods in Applied Mechanics and Engineering*, 195 (2006) 2002-2027.

Solution of Fully-Discretized Equations

Quasi-Direct Coupling

$$\left.\frac{\partial \mathbf{N}_1}{\partial \mathbf{d}_1}\right|_{\left(\mathbf{d}_1^i,\ \mathbf{d}_2^i,\ \mathbf{d}_3^i\right)} \left(\Delta \mathbf{d}_1^i\right) + \left.\frac{\partial \mathbf{N}_1}{\partial \mathbf{d}_2}\right|_{\left(\mathbf{d}_1^i,\ \mathbf{d}_2^i,\ \mathbf{d}_3^i\right)} \left(\Delta \mathbf{d}_2^i\right) = \mathbf{F}_1 - \mathbf{N}_1\left(\mathbf{d}_1^i,\ \mathbf{d}_2^i,\ \mathbf{d}_3^i\right)$$

$$\left.\frac{\partial \mathbf{N}_2}{\partial \mathbf{d}_1}\right|_{\left(\mathbf{d}_1^i,\ \mathbf{d}_2^i,\ \mathbf{d}_3^i\right)} \left(\Delta \mathbf{d}_1^i\right) + \left.\frac{\partial \mathbf{N}_2}{\partial \mathbf{d}_2}\right|_{\left(\mathbf{d}_1^i,\ \mathbf{d}_2^i,\ \mathbf{d}_3^i\right)} \left(\Delta \mathbf{d}_2^i\right) = \mathbf{F}_2 - \mathbf{N}_2\left(\mathbf{d}_1^i,\ \mathbf{d}_2^i,\ \mathbf{d}_3^i\right)$$

$$\left.\frac{\partial \mathbf{N}_3}{\partial \mathbf{d}_3}\right|_{\left(\mathbf{d}_1^{i+1},\ \mathbf{d}_2^{i+1},\ \mathbf{d}_3^i\right)} \left(\Delta \mathbf{d}_3^i\right) = \mathbf{F}_3 - \mathbf{N}_3\left(\mathbf{d}_1^{i+1},\ \mathbf{d}_2^{i+1},\ \mathbf{d}_3^i\right)$$

SELECTIVE SCALING ON 1+2 BLOCK

Ringsail Parachute

Homogenized Modeling of Geometric Porosity (HMGP-FG)

Dynamic Area Changes in FSI

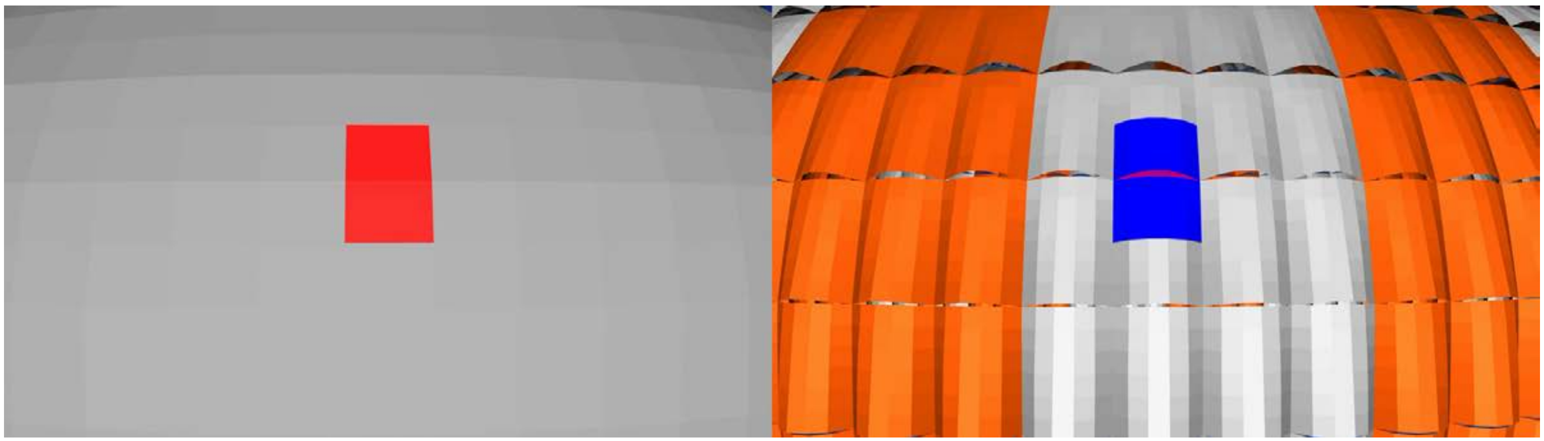

A_1 : Fluid Surface Area

A_F : Fabric Area

A_G : Gap Area

$$u_n = -\left(k_F\right)_J \boxed{\frac{A_F}{A_1}} \Delta p - \left(k_G\right)_J \boxed{\frac{A_G}{A_1}} sgn(\Delta p) \sqrt{\frac{|\Delta p|}{\rho}}$$

HMGP-FG

n-Gore Fluid Mechanics Computation

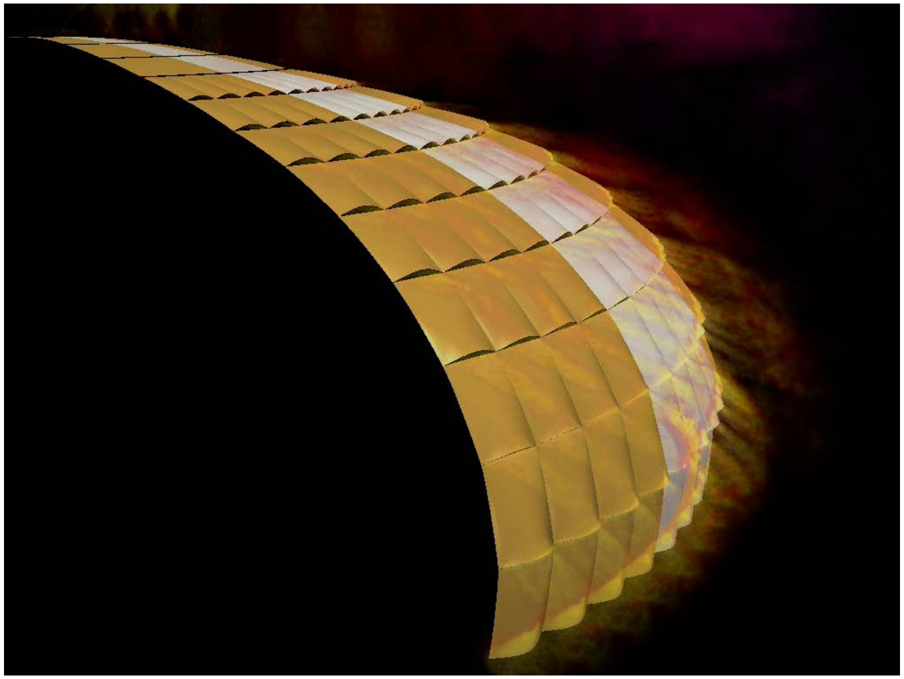

HMGP-FG

Shape Dependency in a Breathing Cycle

Shape varies with breathing:

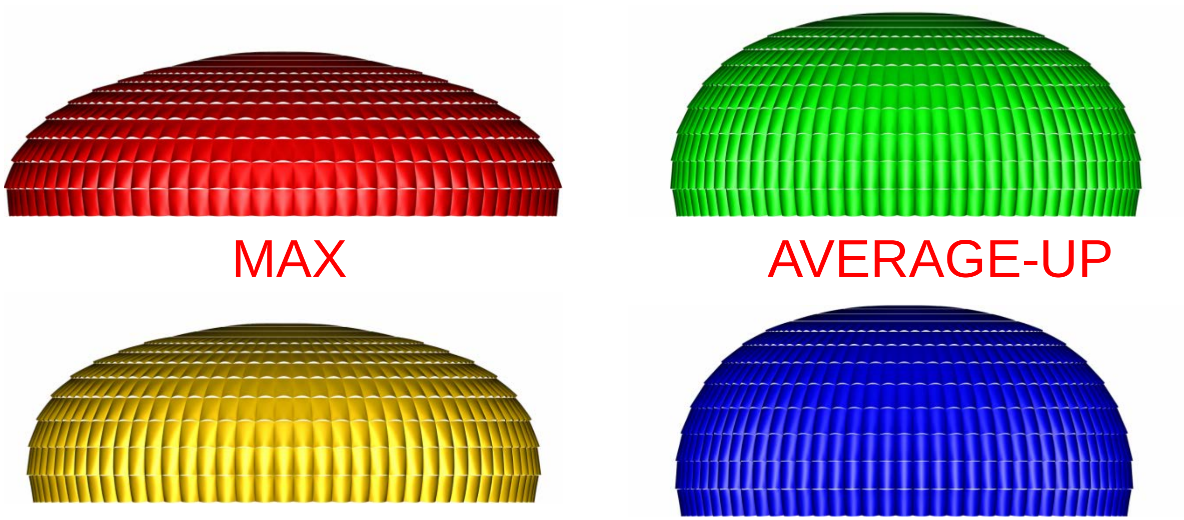

MAX

AVERAGE-UP

AVERAGE-DOWN

MIN

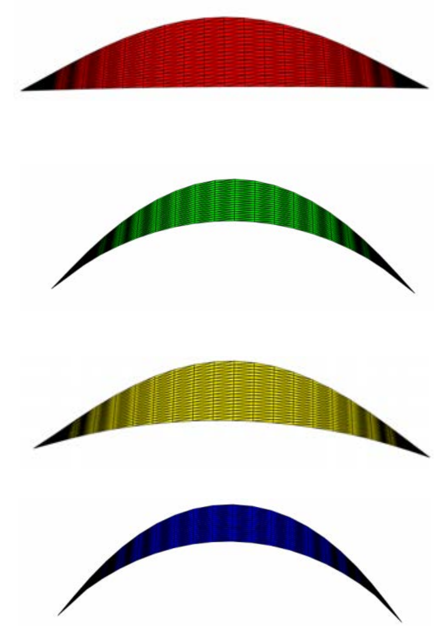

Slit Geometries

Shapes determined by structure-only computation using symmetrized pressure coming from a coarse-mesh FSI.

T★AFSM

FSI Modeling of Spacecraft Parachutes

Opening ("Disreefing") From Stage 2 to Stage 3

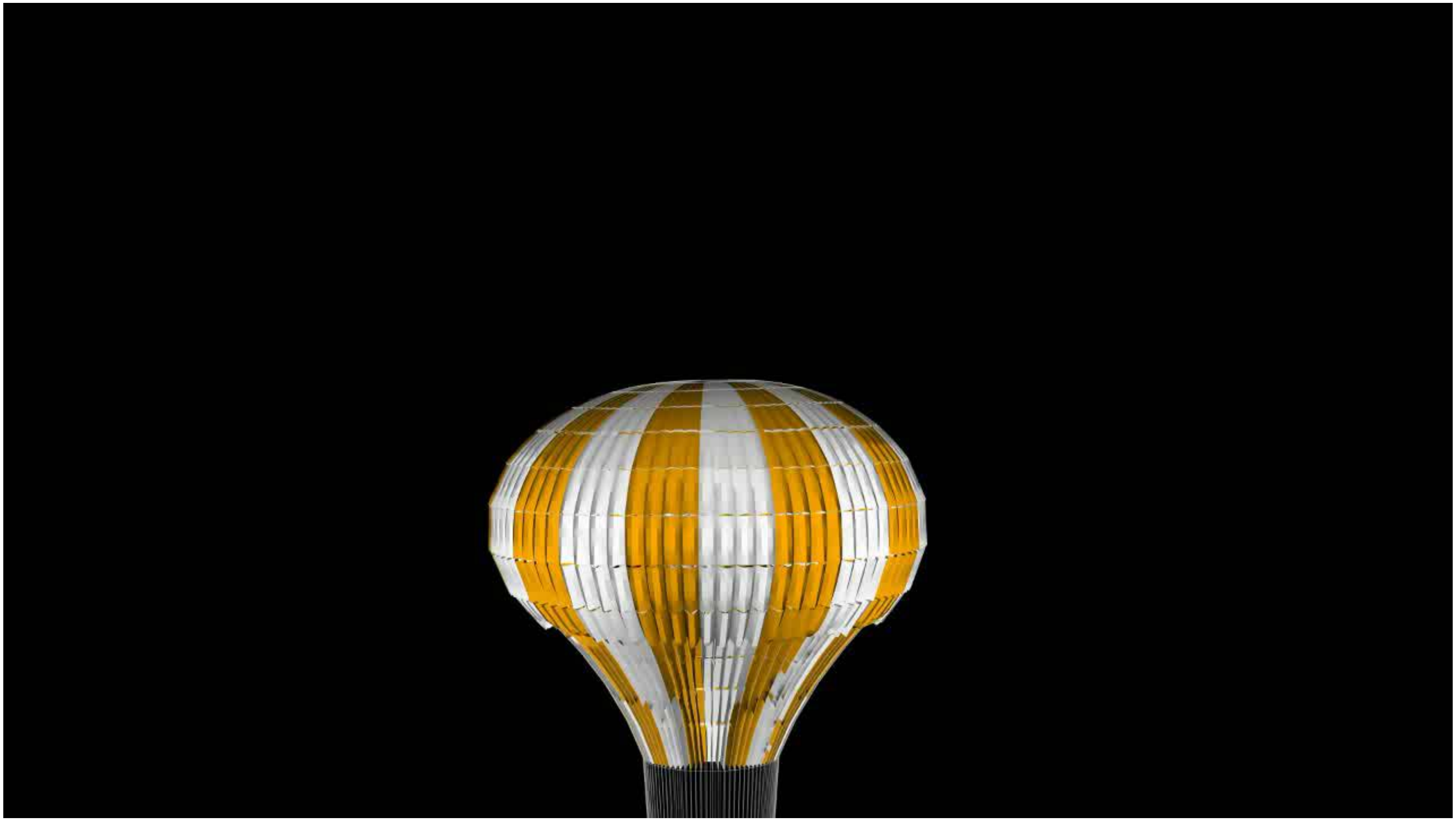

Aerodynamics of Flapping Wings

Smooth-Surface and Motion Representations

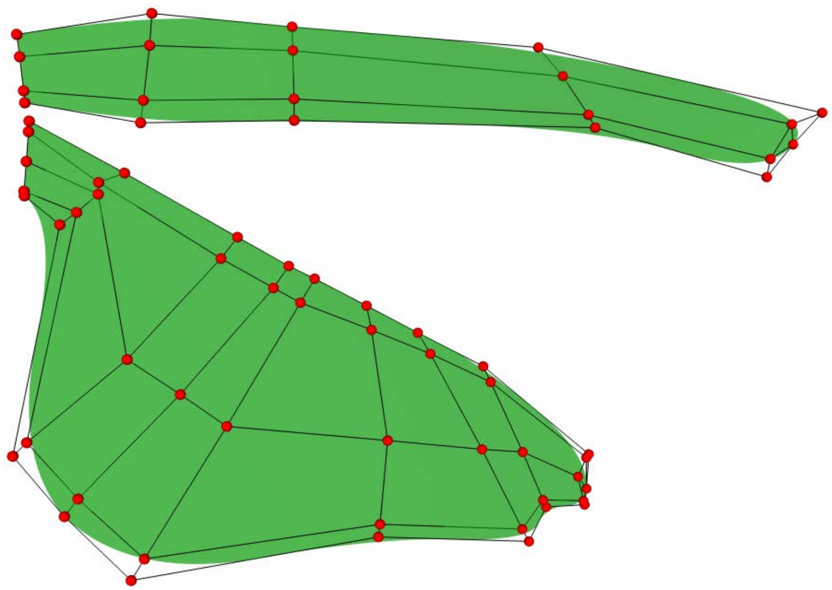

Surface Representation

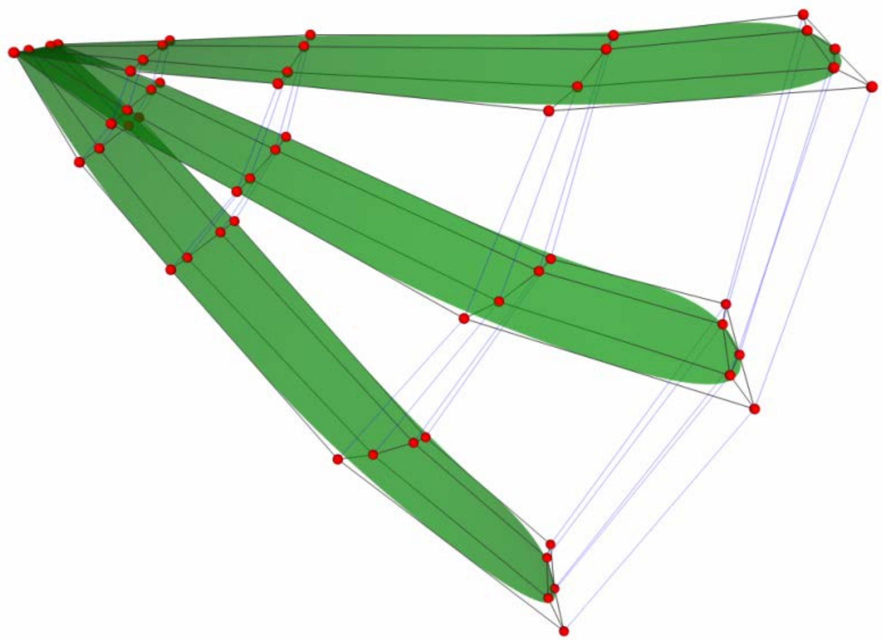

Motion Representation

K. Takizawa, B. Henicke, A. Puntel, T. Spielman and T.E. Tezduyar,
"Space–time computational techniques for the aerodynamics of flapping wings",
Journal of Applied Mechanics, **79**, 010903 (2012).

Solution to Experiment Limitations

- Video-capturing limitations
  - Not enough tracking points
  - Error and uncertainty

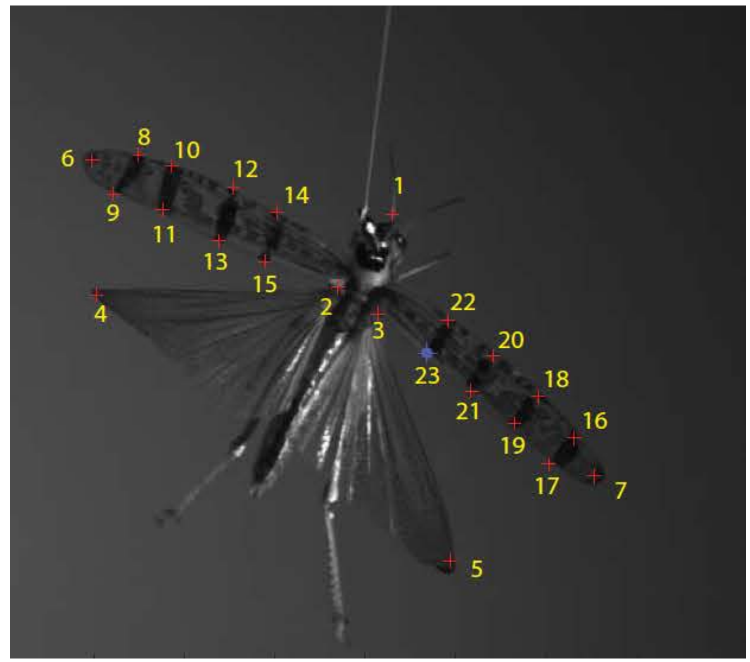

Tracking Points

Dr. Fabrizio Gabbiani and Dr. Raymond Chan (BCM, Houston)

Aerodynamics of Flapping Wings

Actual Locust and Computer Model

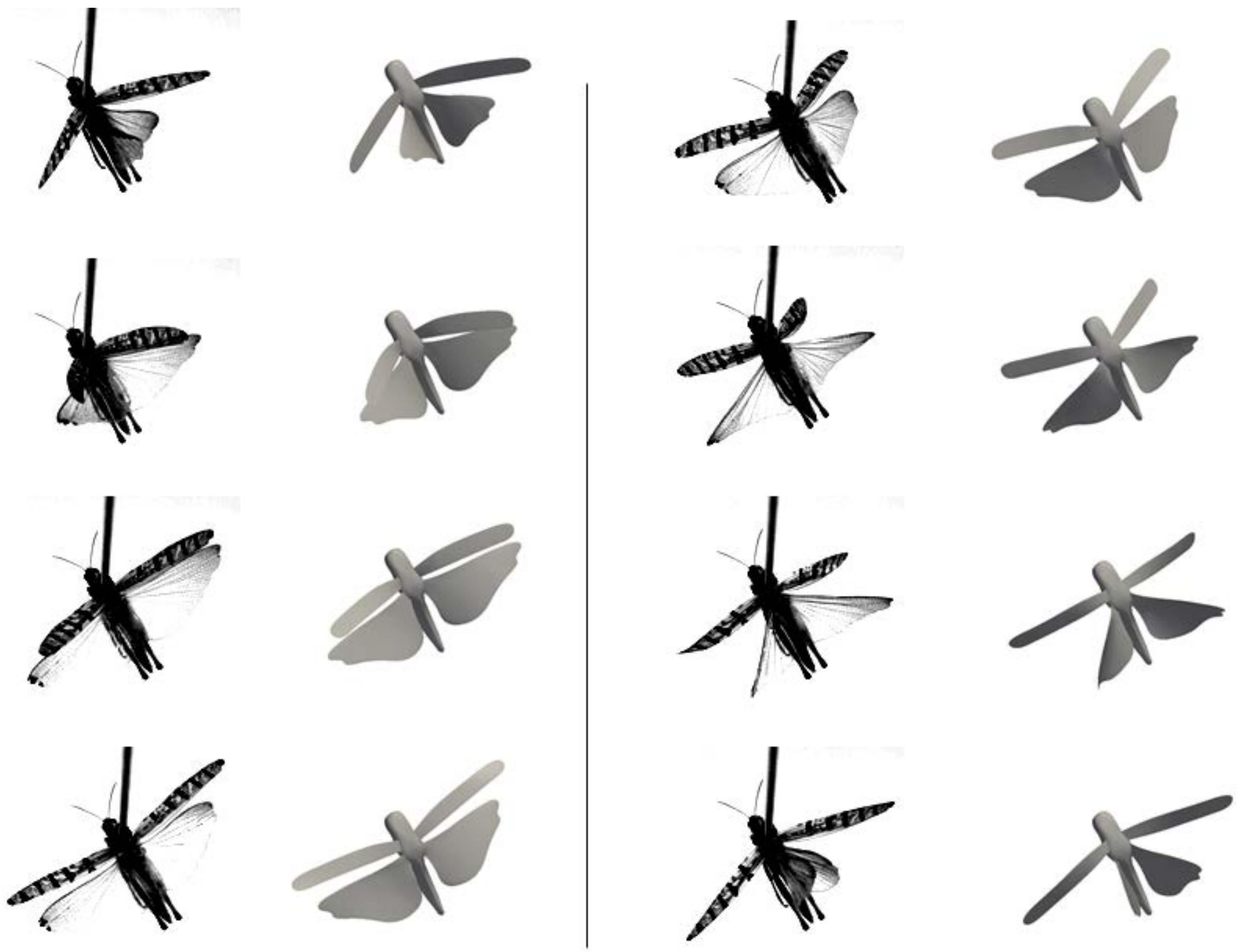

Mesh Moving and Remeshing With NURBS Representation in Time

Mesh Motion

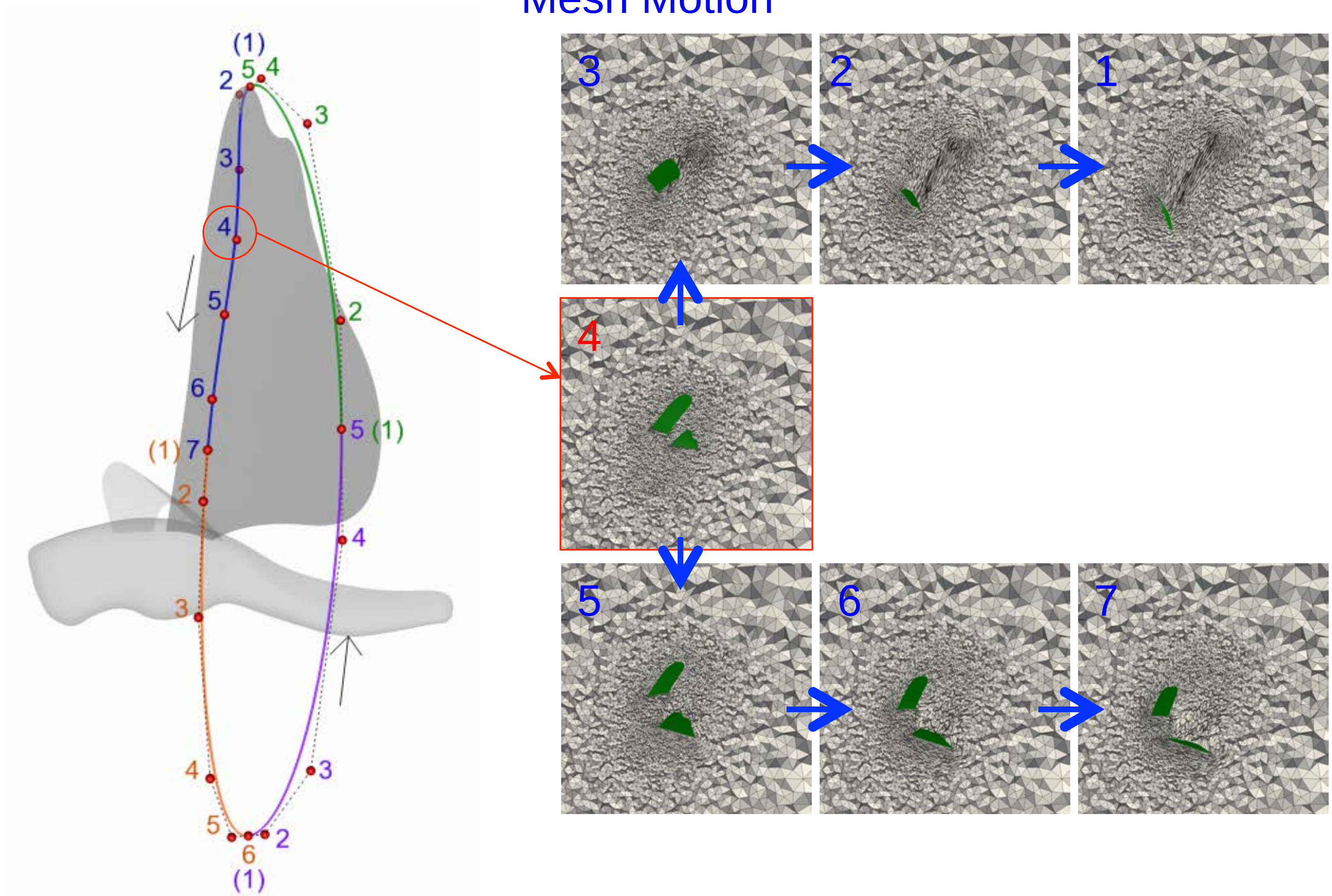

T★AFSM

WIAS RICE